Regeneration of critical bone defects with anionic collagen matrix as scaffolds

Fúlvio Borges Miguel · Aryon de Almeida Barbosa Júnior ·
Fabiana Lopes de Paula · Isabela Cerqueira Barreto ·
Gilberto Goissis · Fabiana Paim Rosa

Abstract The aim of this study was to make a histo-morphometric evaluation of the osteogenic potential of anionic collagen matrix as scaffolds; either crosslinked in glutaraldehyde or not cross-linked and, implanted in critical bone defects in rat calvaria. Seventy-two rats were randomly distributed in three groups: anionic collagen scaffolds treated for 24 h of selective hydrolysis (ACSH); anionic collagen scaffolds treated for 24 h of selective hydrolysis and 5 min of crosslinking in glutaraldehyde 0.05 % (ACSHGA); empty bone defect (Control), evaluated at the biological points of 15, 45, 90 and 120 days. The results showed that the biomaterials implanted were biocompatible and showed a high osteogenic potential. These biomaterials presented a speed of biodegradation compatible with bone neoformation, which was shown to be associated with angiogenesis inside the scaffolds at all biological points. The percentage of mineralization of ACSH (87 %) differed statistically from that found in ACSHGA (66 %). It was concluded that the regeneration of critical bone defect was more evident in anionic collagen without crosslinking (ACSH).

1 Introduction

The researchers of Tissue Bioengineering Area have used biomaterials, cells, and growth factors for creating artificial organs and tissues, or biological substitutes for improving or restoring lost tissue function [1]. Biomaterials of the scaffold type used in the form of a three dimensional (3D) matrix, provide a substrate for the cells migration, proliferation, differentiation, and deposit a new extracellular matrix and form new blood vessels essential for tissue regeneration. According to O'Brien et al. [2] natural scaffolds play an important role in tissue regeneration because they potentially mimic the various functions of extracellular matrix (ECM).

Among the natural polymers used for the manufacture of these 3D matrices, the Type I collagen is widely used as a raw material due to its low antigenicity, its excellent biocompatibility, haemostatic properties, biodegradability and bioreabsorbability [3–6], and presents sites of cell adhesion [5, 7]. However, in same cases, upon implantation in vivo, the biodegradation and the bioabsorption occurs before the biomaterial completes its function [6] because of the enzymatic degradation by collagenases. Therefore, collagen derived-biomaterials require some modifications using a physical or chemical treatment that improves the biochemical and mechanical properties before implantation [4, 6, 8, 9].

The alkaline treatment causes selective hydrolysis of the carboxyamide of asparagine and glutamine present in Type I collagen α-chains, and removes the cells of collagen native [10–12]. During this treatment, the triple helix

F. B. Miguel · A. A. Barbosa Júnior
Gonçalo Moniz Research Center, Oswaldo Cruz Foundation,
Salvador, Bahia, Brazil

F. B. Miguel (✉) · F. L. de Paula
Health Sciences Center of Federal University of the Recôncavo
of Bahia, Avenida Carlos Amaral, 1015, Cajueiro,
Santo Antônio de Jesus, Bahia, Brazil
e-mail: fulviomiguel@yahoo.com.br

I. C. Barreto · F. P. Rosa
Health Sciences Institute of Federal University of Bahia,
Salvador, Bahia, Brazil

G. Goissis
Biotech Biomédica®, São Carlos, Saõ Paulo, Brazil

structure is preserved and the resulting biomaterials present an increased number of negative charges, raised dielectric and piezoelectric properties [3, 8–10, 12–14], lower thermal stability [13, 14] and enhanced the number of cell adhesion sites [15] and pores [16] compared to native collagen.

Another approach to preparing collagenous materials, which could enhance its applicability as a biomaterial, can be the use of glutaraldehyde. This crosslinking reagent has been widely used to stabilize collagen [17–19], reducing immunogenicity and increasing its strength for enzymatic degradation [14, 20]. However, this reagent can release cytotoxic degradation products in the implantation site [6, 21], so it is necessary to test the biomaterials crosslinked in GA before the specific application. Therefore, the aim of this study was to investigate the osteogenic potential of two hydrolysed collagen-based scaffolds, either crosslinked in GA, or not crosslinked, in critical sized defects.

2 Materials and methods

2.1 Experimental model

The experimental procedure was carried out after being approved by the Ethical Committee on Animal Use of Gonçalo Moniz Research Center, Oswaldo Cruz Foundation, in accordance with the guidelines of this committee. Throughout the experiment the animals were kept in individual plastic cages and received solid rations and water *ad libitum*.

Seventy-two male Wistar rats, weighing between 400 and 450 g, 3–5 months old, were randomly distributed in three groups, with six animals in each biologic point of analysis: anionic collagen scaffolds treated by 24 h of selective hydrolysis (ACSH); anionic collagen scaffolds treated for 24 h of selective hydrolysis and 5 min of crosslinking in GA 0.05 % (ACSHGA); empty bone defect without biomaterial implantation (Control). The animals were evaluated at the biological points of 15, 45, 90 and 120 days postoperatively.

2.2 Preparation of biomaterials

The scaffolds evaluated in this study had the shape of a three-dimensional matrix. The materials were prepared and provided by Biotech Biomédica®, manufactured according to Goissis et al. [10], Lacerda et al. [11] and Bet et al. [12]. Fresh bovine pericardium was subjected to selective hydrolysis of side chain amides of asparagine and glutamine for 24 h, as described in Bet et al. [12], Goissis et al. [22], Rosa et al. [8] and Rocha et al. [23]. The biomaterials implanted in ACSHGA were crosslinked in GA 0.05 % for

5 min according to the technique described in Goissis et al. [24] and Goissis et al. [14]. The biomaterials were sterilized with ethylene oxide. Before implantation the lyophilized biomaterials were hydrated in sterile saline solution.

2.3 Surgical procedures and biomaterials implantation

After general anesthesia and analgesia the periosteum was removed and full-thickness critical bone defects were created in the middle portion of the calvaria as described in Cardoso et al. [25] and Miguel et al. [26]. However, in the present study the bone defects were created using a trephine drill with an internal diameter of 8 mm, and outer diameter of 8.5 mm. After removal of the bone disk, the biomaterials with 8.5 mm diameter and 0.8 mm thickness were implanted in the bone defects in ACSH and ACSHGA groups. In the control group, the defects were maintained without biomaterial implantation, and filled with blood coagulum. After these procedures, the soft tissues were repositioned and sutured with silk thread 4.0.

2.4 Histological processing

At 15, 45, 90 and 120 days after the surgical procedures, the animals were sacrificed by CO_2 asphyxiation. The skin and surrounding soft tissues were dissected and the calvaria were removed and cut in half through the center of the bony defect. Subsequently, five specimens were immediately fixed in 70 % alcohol for a minimum of 7 days and embedded in methylmetacrylate resin. These blocks were sectioned using a hard tissue microtome (Leica® RM 2255—Leica Biosystems Nussloch GmbH, Germany), at 6 μm thickness, in the transversal direction of the cranial portion through the center of the circular bone defects without being decalcified.

One specimen for each group and biological point was fixed in a 4 % formalin solution and subsequently decalcified in 7 % nitric acid (2 h) and sent for routine laboratory processing for embedding in paraffin. The blocks were sectioned at 5 μm thickness in the transversal direction of the cranial portion through the center of the circular bone defects.

All histologic cuts were stained with Hematoxylin and Eosin (H.E.), Sirius Red (S.R.) for collagen fibers, Masson-Goldner's Trichrome (T.G.) for the deposition osteoid matrix and analyzed by common light microscopy (Leica®—DM1000, Leica, Biosystems Nussloch GmbH, Germany).

2.5 Histomorphometric assessment

Histomorphometric analysis was performed to quantify, in millimeters, the percentage of linear filling of the defect by

newly formed bone, and the number of blood capillaries in a standard area of 10^6 µm². In this analysis only the cross sectioned capillaries, in which the ratio between the horizontal and vertical diameter did not exceed 20 %, was considered. The morphometric measurements were made using the Leica Qwin Image Processing Analysis System 3.1 (Leica® Microsystems Imaging Solutions, Cambridge, UK). Values were given as mean value (±) standard deviation. To compare the differences between the groups the following tests were used: Mann–Whitney, Linear Regression, Analysis of Variance (ANOVA) with Newman–Keuls post tests, using the software GraphPad Prism®, version 3.1 (GraphPad Software Inc., California, USA), at a 5 % level of significance ($p \leq 0.05$).

3 Results

3.1 Histomorphological analysis

3.1.1 Day 15

In the three experimental groups only a limited chronic inflammation was noted—more inconspicuously in the control group. In the groups ACSH and ACSHGA this inflammatory reaction was of the granulomatous type, with multinucleated giant cells a little more evident in ACSHGA. In the two groups that were implanted with biomaterials, there was a formation of loose connective tissue with a proliferation of fusiform cells and blood capillaries, both within the scaffold between the matrix fibers (Fig. 1a—ACSH) and at the interface between the bone edges and biomaterial. Associated with these biomaterials, the formation of nuclei mineralization in the supradural region was observed (Fig. 1b—ACSH and c—ACSHGA). In the control group, bone formation was observed to be restricted only to the bone edges with the formation of loose connective tissue throughout its cross-sectional area (Fig. 1d—Control).

3.1.2 Day 45

In the control group, the chronic inflammation was shown to be very modest. In the groups ACSH and ACSHGA there remained a presence of chronic granulomatous inflammation, but less prevalent, and seen mainly in the superior region of the matrices, most notably in the ACSHGA group (Fig. 2a—ACSHGA). The collagen fibers of the biomaterial were slightly fragmented in both groups. In ACSH, the mineralized areas, in the majority of instances, occupied two thirds of the biomaterial thickness (Fig. 2b—ACSH) with

scarce bone marrow formation (Fig. 2c—ACSH). In these areas, the fibers of collagen of the biomaterial integrating the mineralized tissue can be observed. In ACSHGA, there was preeminent mineralization along nearly all of the entire linear extent of the defect, notably in the supradural region (Fig. 2d—ACSHGA). Surrounding the nucleus of mineralization in both group ACSH and ACSHGA, active osteoblasts and osteocytes can be observed. In the control group, the bone regeneration continued to be restricted to the defect margins, with the formation of denser fibrous connective tissue in comparison with that observed in the previous period.

3.1.3 Day 90

In ACSH, this reaction was scarce, noted particularly in the periphery of the scaffold. In this group the collagen fibers of the biomaterial presented a residual aspect. In ACSHGA, the chronic granulomatous inflammation remained scarce throughout the extent of the biomaterial, which presented fragmented. Neomineralization was observed throughout the extent of the matrix in both groups. In ACSH, it was observed that the neoformed mineralized tissue filled almost the total matrix thickness (Fig. 3a—ACSH), with vascularization channels and incipient bone marrow formation in the thicker areas. In the areas where there was no neomineralization, there was deposition of connective tissue rich in fusiform cells and blood capillaries (Fig. 3b—ACSH) throughout the cross-sectional area of the defect in both groups. In the control group, inflammation was absent and defect regeneration continued in a similar manner to that in the previous biological point.

3.1.4 120 Days

In ACSH, inflammation was present only in the regions close to the tegumentary flap, where the residual biomaterial fibers were found to be very fragmented. In ACSHGA, the mononuclear inflammatory infiltrate was diffuse and very modest, observed especially in the peripheral areas of the biomaterial, where granulomatous inflammation was noted. Neomineralization in ACSH was more evident when compared to ASCHGA and occupied four fifths of the biomaterial thickness (Fig. 4a—ACSH) with bone marrow and lamella formation. The connective tissue present between the biomaterial and bone edge was mineralized and integrated with the biomaterial at the bone edge. In ACSHGA, mineralization was observed throughout the extent and thickness of the matrices, and showed integration of biomaterial fiber (Fig. 4b—ACSHGA). There was formation of bone marrow and organization in
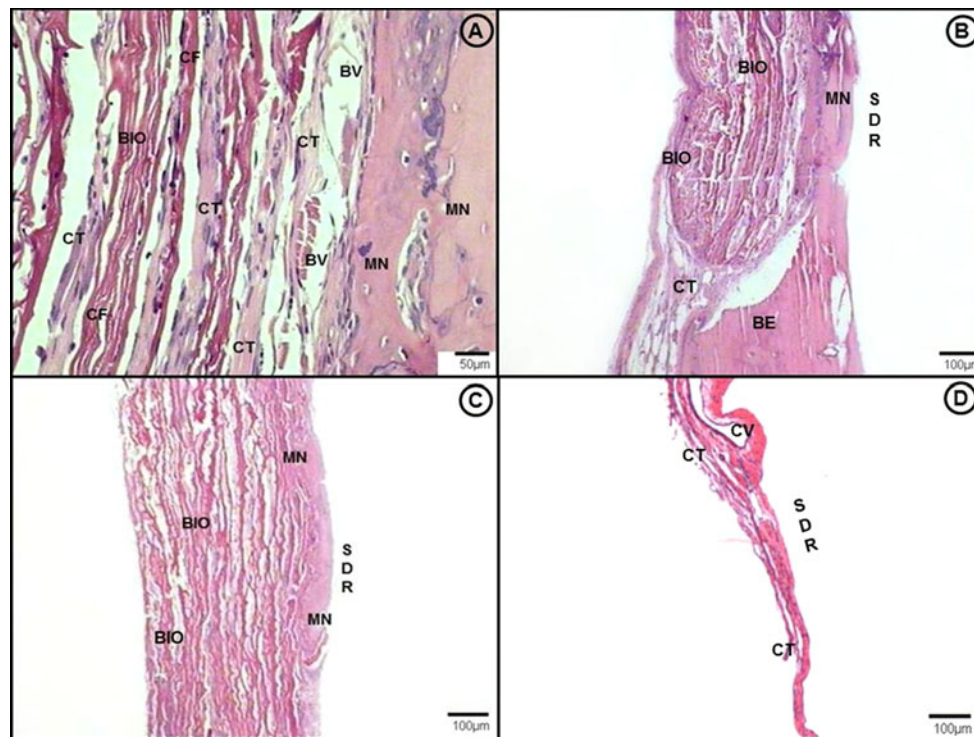
Fig. 1 **a** [ACSH] Formation of connective tissue (*CT*) and blood vessels (*BV*) between the collagen fibers (*CF*) of biomaterial (*BIO*). Mineralization nucleus (*MN*) surrounded by blood vessels and connective tissue. Hematoxylin and Eosin (H.E.); paraffin. **b** [ACSH] Nucleus of mineralization associated with biomaterial in supradural region (*SDR*) near to the bone edge (*BE*). H.E. paraffin. **c** [ACSHGA] Nucleus of mineralization formed in the central region of the defect next supradural region. H.E. paraffin. **d** [Control] Connective tissue formed throughout the length of the defect. Central vein (*CV*). H.E. paraffin

layers around a vascular channel (Fig. 4c—ACSHGA). In the control group, repair of the defects was concluded with the formation of dense connective tissue (Fig. 4d—Control) and bone regeneration restricted to the bone edge.

3.2 Histomorphometric analysis

The linear extent of primary defects showed no statistically significant intra- and inter-group differences throughout the experimental period (data not shown). The morphometric data are shown in Tables 1, 2, and Fig. 5. The percentage of neomineralized tissue in ACSH and ACSHGA, showed a statistically significant increase throughout the times analyzed (linear regression ACSH $p = 0.02$ S and ACSHGA $p = 0.02$ S) among groups ACSH, ACSHGA and control (ANOVA $p = 0.03$ S). When ACSH was compared with ACSHGA (Newman–Keuls $p < 0.05$ S) and ACSHGA with the control (Newman–Keuls $p < 0.05$ S) statistically significant differences were noted. However, in the comparison between ACSH and control the values were stronger statistically significant (Newman–Keuls $p < 0.001$ SS). In the control group, there were no statistically significant differences in the percentage of neomineralized tissue throughout the entire experimental period (linear

regression $p = 0.08$ NS). In this group, the neomineralized tissue did not change significantly over the course of time (Table 1; Fig. 5).

The measurement of neoformed blood capillaries among the matrix fibers showed an increase over the course of time, in spite of the linear regression analysis not having been significant in any one of the groups. Comparison between the means of ACSH and ACSHGA also showed no statistically significant differences (Mann–Whitney $p = 0.11$ NS) (Table 2).

4 Discussion

Based on the biological concepts of bone tissue regeneration, studies evaluating the osteogenic potential of biomaterials should use experimental models that mimic the conditions in which regeneration occurs in a limited manner. On the basis of this premise, the present study evaluated two hydrolyzed anionic collagen matrices, either crosslinked in GA or not crosslinked, and implanted them in critical bone defects in rat calvaria. The histomorphometric results of the control group, in which critical bone defects were maintained without biomaterial implantation,
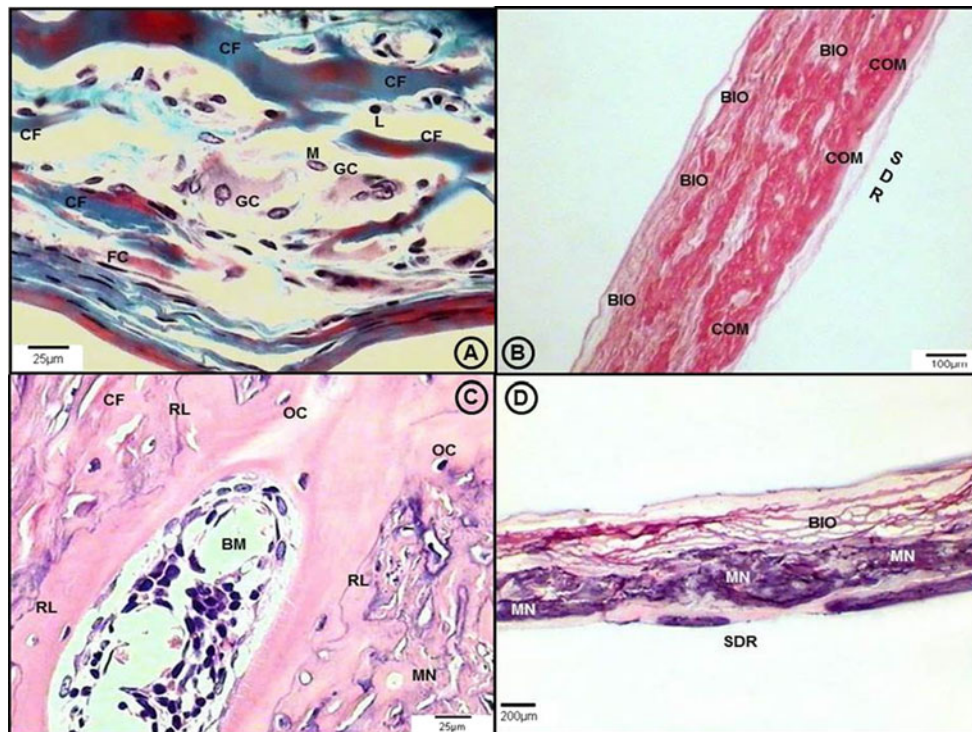
Fig. 2 **a** [ACSHGA] Chronic granulomatous inflammation between the biomaterial fibers; multi-nucleated giant cells (*GC*), lymphocytes (*L*) and macrophages (*M*). Fusiform cell (*FC*). Masson–Goldner's Trichrome (T.G.) resin. **b** [ACSH] Deposition of collagen-rich osteoid matrix (*COM*) filling two thirds of the biomaterial thickness. Sirius Red (S.R.) paraffin. **c** [ACSH] Incipient bone marrow (*BM*) formation in the central area of the defect. Collagen fibers of the biomaterial are shown integrated with newly formed mineralized tissue. Osteocyte (*OC*). Reversion line (*RL*). H.E. paraffin. **d** [ACSHGA] Mineralization along the entire linear extent of the defect, notably in the supradural region. H.E. resin
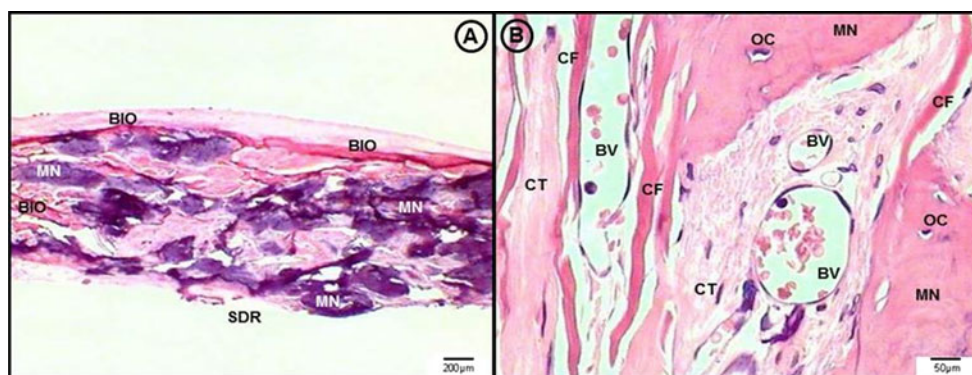

Fig. 3 **a** [ACSH] Neoformed mineralized tissue throughout almost the entire thickness of the biomaterial, with a reticular aspect. H.E. resin. **b** [ACSH] Vascular and connective tissue neoformation in the midst of the biomaterial fibers and mineralization nucleus. H.E. paraffin

showed minimal regeneration which was limited to the edges of the defect with fibrosis formation in the remaining area of the defect (25 % at 120 days). These morphologic findings corroborate the results of Takagi and Urist [27], Schmitz and Höllinger [28], Pang et al. [29], Cardoso et al. [25] and Miguel et al. [26].

The biomaterials evaluated in this study were biocompatible despite having developed discreet chronic inflammatory response. According to Tsai et al. [30], Rosa et al. [8], Anderson et al. [31] a chronic granulomatous inflammation is considered a response inherent to the healing mechanism in biomaterial implantation. In our study, the matrices were submitted to selective hydrolysis. In this treatment, the cells of native collagen were removed [10–12, 16], which probably favored the development of a discreet inflammatory response. When the native cells are present in non-hydrolyzed collagen, the biomaterial develops a more intense inflammatory response [8], which
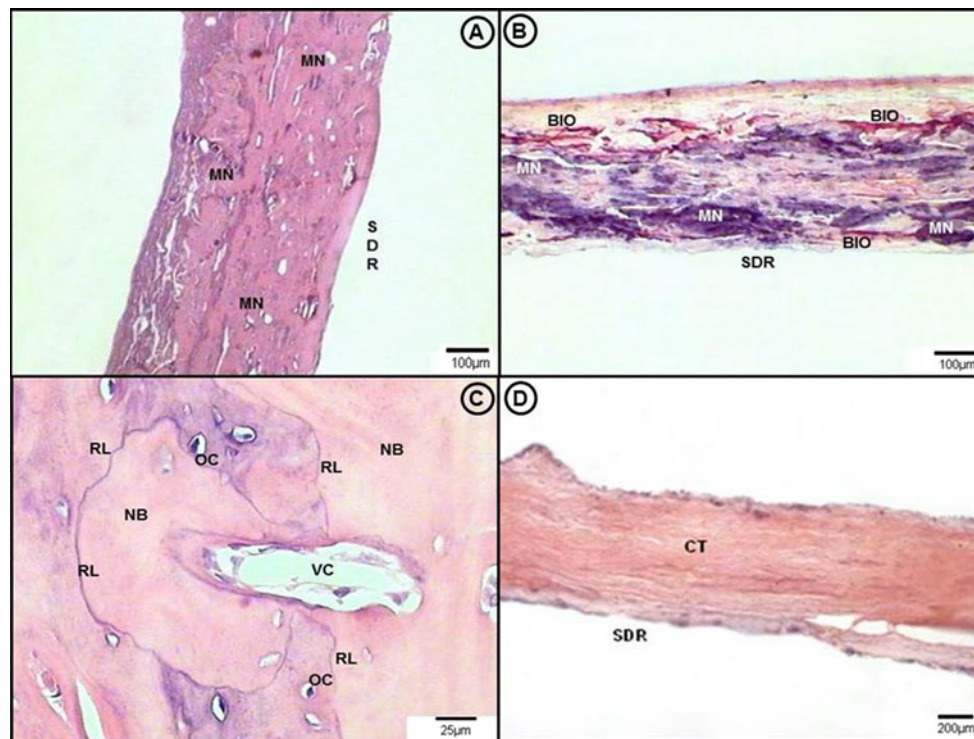
Fig. 4 **a** [ACSH] Extensive area of confluent mineralization nearly the entire thickness of the biomaterial involving collagen fibers of biomaterial. H.E. paraffin. **b** [ACHSGA] Mineralization throughout the extension of the biomaterial, occupying nearly its entire thickness. The fibers of the biomaterial are shown integrating the newly formed mineralized tissue. H.E. resin. **c** [ACSHGA] Neoformed bone (*NB*) tissue organized in layers around a vascular channel (*VC*). H.E. paraffin. **d** [Control] Connective tissue with a dense and organized aspect in the central region of the defect. Note the absence of mineralization. H.E. paraffin

Table 1 Percentage of defect filling by neomineralized tissue, neomineralized cross-sectional area in relation to the total cross-sectional area of the defect

Group	15 days	45 days	90 days	120 days	Linear regression
ACSH	49.0 ± 20 %	66.0 ± 20 %	83.0 ± 10 %	87.0 ± 2 %	$p = 0.02$ S
ACSHGA	23.0 ± 12 %	40.0 ± 16 %	49.4 ± 18 %	66.0 ± 23 %	$p = 0.02$ S
Control	11.7 ± 9 %	21.0 ± 18 %	23.8 ± 17 %	25.4 ± 13 %	$p = 0.08$ NS
ANOVA	ACSH × ACSHGA × Control				$p = 0.03$ S
Newman–Keuls	ACSH × ACSHGA				$p < 0.05$ S
	ACSH × Control				$p < 0.001$ SS
	ACSHGA × Control				$p < 0.05$ S

NS not statistically significant, *S* statistically significant, *SS* stronger statistically significant

may limit the use of the biomaterial. In ACSHGA group this inflammatory response was more evident probably due the crosslinking in GA that reduces the antigenicity of collagen and improves its resistance to enzymatic degradation [20]. However, this agent releases free aldehyde monomers that result in an inflammatory response [32, 33].

The selective hydrolysis provides new microstructural parameters for collagen that can promote new bone formation. Among these are: extra negative charges, an increase in piezoelectric properties [3, 10–12, 16], the removal of native cells and the establishment of pores in the dense structure of the pericardium [16], and an increased number of cell adhesion sites [15]. The presence of anionic loads enabled the insertion of various growth factors [5, 16] and modified conformation of the hydrophobic barrier at the junction gap/overlap, favoring osteogenesis [22]. The neomineralization observed in all the biological points of groups ACSH and ACSHGA could be associated with of presence the pores in the structures of the matrices. The scaffolds evaluated in this study had pores with a mean diameter of 42 μm [16], which enabled the migration of osteoblasts into their structures and were distributed in an arrangement parallel to the orientation of their fibrils. This occurrence is fundamental because the

porosity and its interconnections are essential for tissue regeneration because they allow the diffusion of nutrients [34] and cellular migration and insertion into the vascular scaffold enabling the formation, deposition of extracellular matrix, and osteogenesis. According to Wintermantel et al. [35], O'Brien et al. [2], Arpornmaeklong et al. [36] and O'Brien et al. [37] scaffolds that present pores with diameters ranging between 50 and 150 μm are appropriate for osteogenesis, particularly because they allow the migration of osteoblasts having a size ranging from 10 to 30 μm [38].

The change in the hydrophobic barrier present in the gap/overlap region [15] after selective hydrolysis favored the deposition of calcium and phosphate ions among the tropocollagen fibrils which allowed the neomineralization [22], which can justify bone formation and regeneration of critical defects in our study. The morphometric analysis

Table 2 Number of blood capillaries in an area of 10^6 μm^2

Group	15 days	45 days	90 days	120 days	Linear Regression
Period					
ACSH		80 ± 28	109 ± 24	178 ±153± 49	
$p = 0.19$ NS					
ACSHGA		66 ± 52	60 ± 19	105 ±924± 17	
$p = 0.20$ NS					
Mann–Whitney	ACSH × ACSHGA				$p = 0.11$ NS

NS not statistically significant

showed a statistically significant increase in mineralization occurred in the cross-sectional area of the defect in the course of the studied time, individually for both ACSH and ACSHGA, as well as when ACSH was compared with ACSHGA. The nuclei for mineralization, seen in the midst of the biomaterial fibers in ACSH and ACSHGA were initially formed starting in the region close to the dura mater and expanding in the direction of the superior portion of the scaffolds. According to Gosain et al. [39] this could be explained by the release of growth factors in this region and by the presence of mesenchymal and osteoblast-lineage cells present in this conjunctive membrane which, when duly stimulated, differentiate into active osteoblasts that secrete osteoid matrix, which was not assessed in our study. In group ACSHGA, the cytotoxicity of GA, precipitated by the release of free aldehydes or those adsorbed on the matrix surfaces during their reticulation, possibly set off a more conspicuous inflammatory response with less centripetal cell migration [32], and consequently, less mineralization. This lower cell migration was similar to that observed by Petite et al. [17], when they also evaluated bovine pericardial matrices crosslinked in GA. This crosslinking agent was used to improve the physico-chemical properties of collagen, especially the resistance to enzymatic degradation [17], promoting a controlled degradation while the biomaterial is replaced or integrated into the neoformed tissue. The histological results showed that both biomaterials presented controlled degradation with collagen fibers integrated into the newly formed mineralized tissue. Although the matrix implanted in group ACSH was not crosslinked in GA, its biodegradation was similar
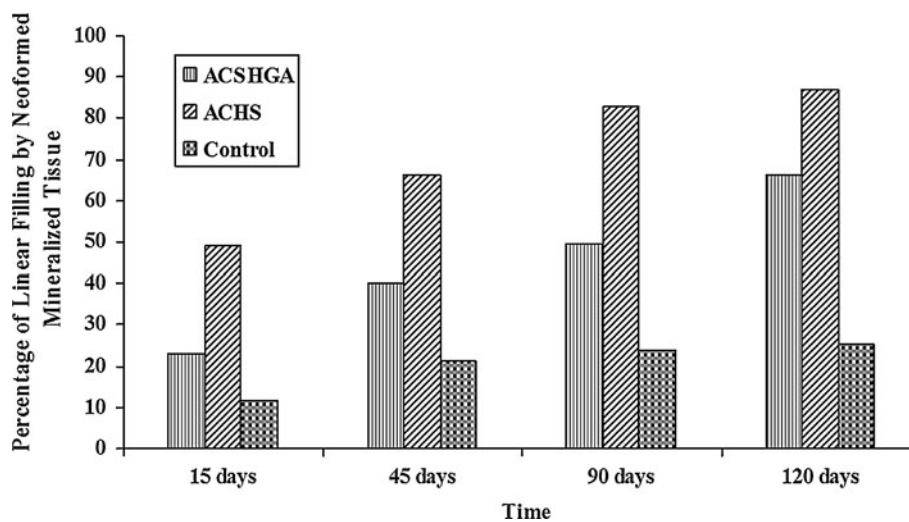

Fig. 5 Analysis of the percentage of neomineralized tissue in the total cross-sectional area of the defect. The graph columns show statistically significant differences among the groups (ANOVA $p = 0.03$ S). Comparison of the groups throughout the experimental period, by means of the linear regression test, pointed out statistically significant differences for groups ACSH ($p = 0.02$ S) and ACSHGA ($p = 0.02$ S), and no significant difference for Group Control ($p = 0.08$ NS). The comparison between groups ACSH and ACS-HGA, as well as between these groups and Control, showed statistically significant differences

to that observed in group ACSHGA. Thus, one can note that the selective hydrolysis itself favored a controlled biodegradation, not requiring crosslinking in GA.

Angiogenesis is an essential mechanism for bone regeneration [40, 41] because the new blood vessels provide cells, oxygen, nutrient [41] and growth factor for the implantation site. In this study, there was evidence of vascular formation in all the biological points studied, which surrounded the nuclei for mineralization in the midst of the matrices fibers. Morphometric analysis showed that this biological event was more evident in ACSH as compared to ACSHGA. Nevertheless, comparison between the means of ACSH and ACSHGA also showed no statistically significant differences. However, there was a correlation between the quantity of neoformed vessels and the percentage of mineralized tissue formed, 87 % in group ACSH and 66 % in group ACSHGA, at 120 days. These findings are in agreement with the observations relative to bone regeneration, which recognize the close connection between vascular formation and osteogenesis [40, 41]. The biomimetic behavior of the studied anionic collagen matrices, with regard to the regeneration of critical defects, has shown evidence of their potential use in future clinical applications.

5 Conclusion

The anionic collagen matrices evaluated in this study were biocompatible and presented a high osteogenic potential for the regeneration of critical bone defects; The reticulation of the anionic collagen matrix in glutaraldehyde does not promote evidence of greater osteogenic potential than matrix without reticulation.

References

1. Ikada Y. Challenges in tissue engineering. J R Soc Interface. 2006;3:589–601.
2. O'Brien FJ, Harley BA, Yannas IV, Gibson LJ. The effect of pore size on cell adhesion in collagen-GAG scaffolds. Biomaterials. 2005;26:433–41.
3. Plepis AMG, Goissis G, Das-Gupta DK. Dielectric and pyroelectric characterization of anionic and native collagen. Pol Eng Sci. 1996;36:2932–8.
4. Lee CH, Singla A, Lee Y. Biomedical applications of collagen. Int J Pharma. 2001;221:1–22.
5. Rocha LB, Brochi MAC, Bellucci AD, Rossi MA. Efficacy of polyanionic collagen matrices for bone defect healing. J Biomed Mater Res B. 2004;71:355–9.
6. Sripriya R, Kumar R, Balaji S, Kumar MS, Sehgal PK. Characterizations of polyanionic collagen prepared by linking additional carboxylic groups. React Funct Polym. 2011;71:62–9.
7. Anselme K. Osteoblast adhesion on biomaterials. Biomaterials. 2000;21:667–81.
8. Rosa FP, Lia RCC, Souza KOF, Goissis G, Marcantonio E Jr. Tissue response to polyanionic collagen: elastin matrices implanted in rat calvaria. Biomaterials. 2003;24:207–12.
9. Cunha MR, Santos AR Jr, Goissis G, Genari SC. Implants of polyanionic collagen matrix in bone defects of ovariectomized rats. J Mater Sci Mater Med. 2008;19:1341–8.
10. Goissis G, Piccirili L, Goes JC, Plepis AMG, Das-Gupta DK. Anionic collagen: polymer composites with improved dielectric and rheological properties. Artif Organs. 1998;22:203–9.
11. Lacerda C, Plepis AMG, Goissis G. Hidrólise seletiva de carboxiamidas de resíduos de asparagina e glutamina em colágeno: preparação e caracterização de matrizes aniônicas para uso como biomateriais. Quim Nova. 1998;21:267–71.
12. Bet MR, Goissis G, Lacerda CA. Characterization of polyanionic collagen prepared by selective hydrolysis of asparagines and glutamine carboxyamide side chains. Biomacromolecules. 2001; 2:1074–9.
13. Góes JC, Figueiró SD, Paiva JAC, Vasconcelos IF, Sombra ASB. On the piezoelectricity of anionic collagen films. J Physics Chem Solids. 2002;63:465–70.
14. Goissis G, Giglioti AF, Braile DM. Preparation and characterization of an acellular bovine pericardium intended for manufacture of valve bioprostheses. Artif Organs. 2011;35:484–9.
15. Bet MR, Goissis G, Vargas S, Selistre-de-Araujo HS. Cell adhesion and cytotoxicity studies over polyanionic collagen surfaces with variable negative charge and wettability. Biomaterials. 2003;24:131–7.
16. Rocha LB, Goissis G, Rossi MA. Biocompatibility of anionic collagen matrix as scaffold for bone healing. Biomaterials. 2002;23:449–56.
17. Petite H, Duval JL, Frei V, Abdul-Malak N, Sigot-Luizard MF, Herbage D. Cytocompatibility of calf pericardium treated by glutaraldehyde and by the acyl azide methods in an organotypic culture model. Biomaterials. 1995;16:1003–8.
18. Khor E. Methods for the treatment of collagenous tissues for bioprostheses. Biomaterials. 1997;18:95–105.
19. Angele P, Abke J, Kujat R, Faltermeier H, Schumann D, Nerlich M, Kinner B, Englert C, Ruszczazak Z, Mehrl R, Mueller R. Influence of different collagen species on physico-chemical properties of crosslinked collagen matrices. Biomaterials. 2004; 25:2832–41.
20. Charulatha V, Rajaram A. Influence of different crosslinking treatments on the physical properties of collagen membranes. Biomaterials. 2003;24:759–67.
21. Gratzer PF, Santerre JP, Lee JM. Modulation of collagen proteolysis by chemical modification of amino acid side-chains in acellularized arteries. Biomaterials. 2004;25:2081–94.
22. Goissis G, Maginador SVS, Martins VCA. Biomimetic mineralization of charged collagen matrices: in vitro and in vivo study. Artif Organs. 2003;27:437–43.
23. Rocha LB, Adam RL, Leite NJ, Metze K, Rossi MA. Biomineralization of polyanionic collagen-elastin matrices during cavarial bone repair. J Biomed Mater Res Part A. 2006;79:237–45.
24. Goissis G, Marcantonio E Jr, Marcantonio RAC, Lia RCC, Cancian DCJ, Carvalho WM. Biocompatibility studies of anionic collagen membranes with different degree of glutaraldehyde cross-linking. Biomaterials. 1999;20:27–34.
25. Cardoso AKMV, Barbosa AA Jr, Miguel FB, Marcantonio E Jr, Farina M, Soares GDA, Rosa FP. Histomorphometric analysis of tissue responses to bioactive glass implants in critical defects in rat calvaria. Cell Tissues Organs. 2006;184:128–37.

26. Miguel FB, Cardoso AKMV, Barbosa Junior AA, Marcantonio E Jr, Goissis G, Rosa FP. Morphological assessment of the behavior of three-dimensional anionic collagen matrices in bone regeneration in rats. J Biomed Mater Res B. 2006;78:334–9.

27. Takagi K, Urist MR. The reaction of the dura to bone morphogenetic protein (BMP) in repair of skull defects. Ann Surg. 1982;196:100–9.

28. Schmitz JP, Höllinger JO. The critical size defect as an experimental model for craniomandibulofacial nonunions. Clin Orthop Relat Res. 1986;225:299–308.

29. Pang EK, Im SU, Kim C, Choi SH, Chai JK, Kim CK, Ham SB, Cho KS. Effect of recombinant human bone morphogenetic protein-4 dose bone formation in a rat calvarial defect model. J Periodontal. 2004;75:1364–70.

30. Tsai AT, Rice J, Scatena M, Liaw L, Ratner BD, Giachelli CM. The role of osteopontin in foreign body giant cell formation. Biomaterials. 2005;26:5835–43.

31. Anderson JM, Rodriguez A, Chang DT. Foreign body reaction to biomaterials. Semin Immunol. 2008;20:86–100.

32. Speer DP, Chvapil M, Eskelson CD, Ulreich J. Biological effects of residual glutaraldehyde in glutaraldehyde-tanned collagen biomaterials. J Biomed Mater Res. 1980;14:753–64.

33. Courtman DW, Pereira CA, Kashef V, McComb D, Lee JM, Wilson GJ. Development of a pericardial acellular matrix biomaterial: biochemical and mechanical effects of cell extraction. J Biomed Mater Res. 1994;28:655–66.

34. Weng J, Wang M. Producing chitin scaffolds with controlled pore size and interconnectivity for tissue engineering. J Mater Sci Mater Med. 2001;12:855–60.

35. Wintermantel E, Mayer J, Blum J, Eckert KL, Lüscher P, Mathey M. Tissue engineering scaffolds using superstructures. Biomaterials. 1996;17:83–99.

36. Arpornmaeklong P, Suwatwirote N, Pripatnanont P, Oungbho P. Growth and differentiation of mouse osteoblasts on chitosancollagen sponges. Int J Oral Maxillofac Surg. 2007;36:328–37.

37. O'Brien FJ, Harley BA, Waller MA, Yannas IV, Gibson LJ, Prendergast PJ. The effect of pore size on permeability and cell attachment in collagen scaffolds for tissue engineering. Technol Health Care. 2007;15:3–17.

38. Aronow MA, Gerstenfeld LC, Owen TA, Tassinari MS, Stein GS, Lian JB. Factors that promote progressive development of the osteoblast phenotype in cultured fetal rat calvaria. J Cell Physiol. 1990;143:213–21.

39. Gosain AK, Santoro TD, Song LS, Capel CC, Sudhakar PV, Matloub HS. Osteogenesis in calvarial defects: contribution of the dura, the pericranium, and the surrounding bone in adult versus infant animals. Plastic Reconstr Surg. 2003;112:515–27.

40. Carano AD, Filvaroff EH. Angiogenesis and bone repair. Drug Discov Today. 2003;8:980–4.

41. Hankenson KD, Dishowitz M, Gray C, Schenker M. Angiogenesis in bone regeneration. Injury. 2011;42:556–61.